



Influence of experimental parameters on in vitro human skin permeation of Bisphenol A

E. Reale^a, A. Berthet^a, P. Wild^{a,b}, D. Vernez^a, N.B. Hopf^{a,*}

^a Center for Primary Care and Public Health (Unisanté), affiliated to University of Lausanne, Route de la Corniche 2, 1066 Epalinges-Lausanne, Switzerland

^b French Research and Safety Institute (INRS), 1 rue du Morvan, CS 60027, F-54519 Vandœuvre cedex, France

ARTICLE INFO

Keywords:

BPA
Percutaneous absorption
Human skin
Skin thickness
Vehicle volume
Permeation constant

ABSTRACT

Bisphenol A (BPA) in vitro skin permeation studies have shown inconsistent results, which could be due to experimental conditions. We studied the impact of in vitro parameters on BPA skin permeation using flow-through diffusion cells with ex-vivo human skin (12 donors, 3–12 replicates). We varied skin status (viable or frozen skin) and thickness (200, 400, 800 μm), BPA concentrations (18, 250 mg/l) and vehicle volumes (10, 100 and 1000 $\mu\text{l/cm}^2$). These conditions led to a wide range of BPA absorption (2%–24% after 24 h exposure), peak permeation rates ($J = 0.02\text{--}1.31 \mu\text{g/cm}^2/\text{h}$), and permeability coefficients ($K_p = 1.6\text{--}5.2 \times 10^{-3} \text{ cm/h}$). This is the first time steady state conditions were reached for BPA aqueous solutions in vitro (1000 $\mu\text{l/cm}^2$ applied at concentration 250 mg/l). A reduction of the skin thickness from 800 and 400 μm to 200 μm led to a 3-fold increase of J ($P < 0.05$). A reduction of the vehicle volume from 1000 to 100 led to a 2-fold decrease in J ($P > 0.05$). Previously frozen skin led to a 3-fold increase in J compared to viable skin ($P < 0.001$). We found that results from published studies were consistent when adjusting J according to experimental parameters. We propose appropriate J values for different exposure scenarios to calculate BPA internal exposures for use in risk assessment.

1. Introduction

Bisphenol A (BPA) is a high production volume chemical (OECD, 2003) with endocrine disruptive effects (Peretz et al., 2014). It is primarily used in polycarbonate plastics such as food and drink containers, as well as in tin cans with epoxy resin lining. Food and drinks in contact with BPA-containing materials are the major source of BPA exposure (EFSA, 2015). In March 2015, the European Food Safety Authority (EFSA) Panel for Food Contact Materials, Enzymes, Flavourings and Processing Aids (CEF) gave a Scientific Opinion on public health risks related to the presence of BPA in foodstuff. It concluded that there is no health concern for any age group from dietary exposure, but noted considerable uncertainty in the exposure estimates for non-dietary sources (EFSA, 2015). Indeed, exposure from food alone cannot explain reported BPA blood and urine concentrations (Mielke and Gundert-Remy, 2009; Völkel et al., 2002). This underestimation of exposure could potentially be due to additional routes of absorption such as the skin contributing to the overall human exposure to BPA.

The second largest BPA source of exposure is thermal paper used in receipts, labels and tickets, where BPA is used as a color developer

(EFSA, 2015). Upon handling, BPA migrates from the thermal paper onto the skin and can be absorbed (Biedermann et al., 2010) or ingested due to hand-to-mouth transfer (Hormann et al., 2014). Skin exposure could contribute significantly to overall BPA body burden. Contrary to ingested BPA, skin absorbed BPA does not undergo first-pass metabolism but goes directly into the systemic circulation (Gundert-Remy et al., 2013). Ndaw et al. (2016) reported that cashiers handling thermal paper receipts daily had higher urinary BPA concentrations compared to non-occupationally exposed workers.

Estimated in vitro BPA skin permeation studies have shown inconsistent results, which could be due to experimental conditions (Champmartin et al., 2020; Demierre et al., 2012; Kaddar et al., 2008; Liu and Martin, 2019; Marquet et al., 2011; Mørck et al., 2010; Toner et al., 2018; Zalko et al., 2011). These studies reported different results for total absorbed BPA (epidermis + dermis + receptor fluid) ranging between 18% (Toner et al., 2018) and 87% (Zalko et al., 2011). Skin permeation kinetics were assessed in five of these studies, which report peak permeation rates (J , $\mu\text{g/cm}^2/\text{h}$) ranging four orders of magnitude between 3.0×10^{-5} and $7.0 \times 10^{-1} \mu\text{g/cm}^2/\text{h}$ (see Table 1). These values were obtained in finite dose experiments where the permeation

* Corresponding author.

E-mail address: Nancy.Hopf@unisante.ch (N.B. Hopf).

<https://doi.org/10.1016/j.tiv.2021.105129>

Received 4 December 2020; Received in revised form 1 February 2021; Accepted 25 February 2021

Available online 1 March 2021

0887-2333/© 2022 The Authors. Published by Elsevier Ltd. This is an open access article under the CC BY license (<http://creativecommons.org/licenses/by/4.0/>).

rate, also called flux, was not constant, but increased to a peak (J_{peak}) before progressively decreasing (Kasting, 2001). In infinite dose experiments, the permeant on the skin is not depleted. Infinite dose permeation rates reach a maximum constant value (steady state) described by Fick's first law of diffusion:

$$J_{\text{ss}} = K_p \times C$$

where J_{ss} represents the diffusion of a mass per unit time and exposed membrane area, K_p is the permeability coefficient (cm/h), a kinetic parameter unique to the test substance, and C is the concentration of the substance in the solution applied on the membrane.

BPA skin absorption did not reach the steady state in any of these previous studies. Liu and Martin (2019) reported a K_p value for BPA in water; however, a decrease in J after 11 h of exposure suggest that steady state was not reached in their study.

Due to these inconsistencies, no overall conclusion can be made concerning BPA's permeation through human skin. Consequently, a range of different skin permeation values has been used in risk assessments (ANSES, 2013; EFSA, 2015) and in toxicokinetic models (Karrer et al., 2018; Mielke and Gundert-Remy, 2012). The CEF Panel is seeking more data on BPA toxicokinetics to reduce the uncertainty regarding skin absorption in BPA hazard assessments (EFSA, 2018).

The differences in published BPA skin permeation data are probably due to different experimental parameters. The Organisation for Economic Co-operation and Development (OECD) Test Guideline 428 (OECD, 2004a), Guidance Document 28 (OECD, 2004b) and Guidance Notes 156 (OECD, 2011) allow skin permeation laboratories the flexibility to adapt several experimental parameters to their research purposes. However, this flexibility makes it difficult to compare results across studies.

The aim of this study was to assess the influence of different

experimental parameters on BPA skin permeation kinetics based on the hypothesis that the same experimental setups should lead to the same results. The main experimental parameters that can affect skin permeation are skin state (viable and frozen), vehicle volume (volume of BPA solution applied on the skin), concentration of the dosing solution applied on the skin, and skin thickness. We thus focused our experimental design on these parameters.

2. Methods

2.1. Materials and chemicals

BPA was purchased from Sigma-Aldrich Chemie GmbH, Buchs, Switzerland. HPLC-grade acetonitrile and water were obtained by Sigma-Aldrich Chemie GmbH, Buchs, Switzerland. Physiological saline solution (saline) was prepared dissolving 0.9% (w/v) sodium chloride (purissim. p.a. $\geq 99.5\%$, supplied by Sigma-Aldrich Chemie GmbH, Buchs, Switzerland) in Milli-Q® water (Milli-Q® Advantage ultra-pure water system, Millipore, Milford, MA, USA). BPA dosing solutions were prepared at different BPA concentrations (18, 164, 250 mg/l) in MilliQ water. The 250 mg/l concentration was based on the reported range of BPA water solubility values (120–300 mg/l, source: US EPA (2014)), 164 mg/l concentration was chosen for comparison with one published article on BPA skin permeation (Demierre et al., 2012), and 18 mg/l was a third value to test the effect of concentration on BPA kinetics. BPA was soluble in both donor and receptor fluids at the tested concentrations as required by the OECD guidelines. The maximum BPA concentration in water was 250 mg/l, which was reached only after sonicating the solution for 1 h and leaving it for 24 h. This solution was considered saturated and was within the reported water solubility values.

Table 1

Experimental setup and results of BPA ex vivo human skin permeation kinetics studies in the literature.

| Authors | Marquet et al., 2011 | Demierre et al., 2012 | Toner et al., 2018 | Liu and Martin, 2019 | Champmartin et al., 2020 |
|--|--|-------------------------------|---|--|--|
| Skin parameters | | | | | |
| Skin thickness (μm) | 400 | 200 | 350–400 | 120 | 476 \pm 56 |
| Skin status | Frozen | Frozen | Viable | 3D model with metabolic activity | Viable |
| Skin anatomical location | NA | Dorsal part of upper leg | Abdomen | Human skin model | Abdomen |
| Methods | | | | | |
| System | Static diffusion cells | Flow through-diffusion cells | Flow through-diffusion cells, 12-well plate for metabolism | Static diffusion device in 6-well plates | Static diffusion cells |
| BPA concentration (mg/l) | 4000 | 194 ^a | 300, 60, 12, 2.4 | 5, 1 | 400 |
| Vehicle | Acetone | Water | Phosphate buffered saline (PBS) | Water | Water, Acetone, Sebum |
| Vehicle volume ($\mu\text{l}/\text{cm}^2$) | 50 | 9.4 | 10 | 1538 | 50 |
| BPA dose ($\mu\text{g}/\text{cm}^2$) | 200 | 1.82 | 3, 0.6, 0.12, 0.024 | 7.7, 1.5 | 20 |
| Receptor fluid | RPMI ^b , 2% BSA ^b , 1% penicillin/streptomycin | Physiological saline solution | DMEM ^b + 1% ethanol + UDPGA ^b 2 mM + PAPS ^b 40 μM | PBS ^b | RPMI 1640 solution +0.2% gentamycin +2.5% penicillin–streptomycin +2% BSA ^b |
| Exposure time (h) | 24 | 24 | 24 | 25 | 24 |
| Results | | | | | |
| J ($\mu\text{g}/\text{cm}^2/\text{h}$) | 0.12 | 0.022 | 3.4E-03, 0.48E-03, 0.14E-03, 0.03E-03 ^c | 0.163, 0.036 ^d | 0.70, 0.0372, 0.0186 ^e |
| K_p (cm/h) | NA | NA | NA | 0.033, 0.036 ^d | NA, 9.3E-05, 4.65E-05 ^e |

NA, not available.

^a BPA-¹³C₁₂ concentration, equivalent to 184 mg BPA/l.

^b Acronyms: RPMI Rosewell Park Memorial Institute medium, BSA bovine serum albumin, DMEM Dulbecco's Modified Eagle Medium, UDPGA Uridine 5'-diphosphoglucuronic acid, PAPS 3'-phosphoadenosine-5'-phosphosulfate, PBS Phosphate buffered saline.

^c Values corresponding to the 300, 60, 12, and 2.4 mg/l dosing solutions, respectively.

^d Values corresponding to the 5 and 1 mg/l dosing solution, respectively.

^e Values corresponding to water, acetone, and sebum vehicle, respectively. For BPA applied in acetone and sebum reported values are J_{ss} .

2.2. Skin permeation assays

Skin permeation studies were carried out in agreement with the OECD guideline 428 (OECD, 2004a). Skin permeation was assessed through viable human skin using a 9-cell jacketed flow-through diffusion cell system (PermeGear® obtained from SES Analytical System, Bechenheim, Germany). Saline was pumped (50 µl/min; peristaltic pump from Ismatec IPC-N, IDEX Health and Science GmbH, Wertheim-Mondfeld, Germany) through the receptor chamber. Cells were kept at 32 °C by a heated water-bath circulator (Haake SC 100 Digital Immersion Circulator, 100 °C w/cla, Thermo Scientific, Newington, NH, USA). Full thickness human abdominal skin was obtained immediately following surgery from the Plastic and Reconstructive Surgery Department (DAL) at the Centre Hospitalier Universitaire Vaudois (CHUV, Lausanne, Switzerland) (ethical protocol 264/12). Patients' data were kept anonymous except for gender and age. Number of donors and replicates varied considerably from one experiment to the other because it depended on the availability of the skin from the Plastic and Reconstructive Surgery Department on experimental days. Skin was rinsed with saline and dermatomed (Acculan®II, B. Braun/Aesculap, Sempach, Switzerland) at 800, 400 or 200 µm. The skin thickness used in each experiment is listed in Table 2. Then skin was cut into circular sections to fit the flow-through diffusion cells (11.28 mm diameter, 1 cm² area). These skin flaps were mounted onto the flow-through diffusion cells with the stratum corneum facing up and left to stabilize for 30-min. No more than two hours elapsed from retrieving to mounting the skin onto the cells. Transepidermal water loss (TEWL) (VapoMeter wireless, Delfin Technologies Ltd., Kuopio, Finland) was measured for each skin flap to assess skin sample integrity (Bronaugh and Maibach, 2005). Skin samples with a TEWL greater than 11 g/m²/h were excluded (Pinnagoda et al., 1990). Skin samples were exposed to different volumes of BPA test preparations at different concentrations for 24 h.

In order to facilitate comparison, several parameters used in our experiments were the same as a previously published article on BPA skin permeation (Demierre et al., 2012): flow-through system, use of aqueous solution as vehicle to apply BPA on the skin, use of saline as receptor fluid, receptor fluid's flow rate, frequency and number of collecting times. Parameters that varied from Demierre et al. (2012) were namely skin state, skin thickness, vehicle volume, and BPA concentration in the test preparation. The different parameters used for each experiment are listed in Table 2. Frozen skin (EXP2 in Table 2) refers to previously frozen skin that had been frozen (− 80 °C) immediately after dermatoming, stored for up to six months, and thawed at room temperature before testing. In all experiments, receptor fluid was sampled by a fraction collector (FC 204, Gilson Inc., Middleton, WI, USA) at specific time intervals up to 24 h. Dosing solution was removed from donor chambers with a pipette and skin surfaces were wiped with cotton swabs and paper tissues at the end of the experiments where 1000 µl were applied. This was not necessary for experiments with volumes smaller than 1000 µL as these skin samples were already dry after 24 h. TEWL was tested again at the end of each experiment to confirm skin integrity

throughout the whole experiment. Methods and results of EXP5 in Table 2 have been previously described (Reale et al., 2020). Briefly, experimental conditions were identical to those described for EXP6 in Table 2 except for vehicle volume (100 µl instead of 1000 µl).

2.3. Sample assays

BPA concentrations in the receptor fluid samples were quantified by high-performance liquid chromatography coupled with fluorescence detection (HPLC-FLD). Samples were filtered with 4-mm syringe filters (PTFE 0.45 µm, BGB Analytik) and then injected into the HPLC. The HPLC was equipped with the following: a pump (Prostar 240, Varian Inc.) pumping HPLC-grade acetonitrile (A) and water (B) in gradient mode at 0.5 ml/min; an auto-sampler (Prostar 410, Varian Inc.) injecting 10 µl sample; a packed column (Accucore™ Phenyl-X column 150 mm × 4.6 mm I.D., 2.6 µm, Thermo Scientific) heated at 30 °C; a fluorescence detector (Prostar 363, Varian Inc.) set at an excitation wavelength of 225 nm and an emission wavelength of 306 nm. The gradient program started with 60:40 A:B (v/v) and increased linearly to 98:2 A:B from 0 to 5 min. This condition was held until 8.5 min. From 8.5 to 9 min, the elution program returned to the initial condition and then held until 13 min. Under these conditions, BPA's retention time was 4.55 min. The calibration standards were prepared in saline, over the range 1.95–500 µg/l, where linearity was ensured (mean R² = 0.999). Calibration curves were calculated by linear regression of the peak area subtracted of the blank peak area, plotted over the nominal concentration for each calibration standard. A value equal to zero was used for each sample concentration under the lower limit of quantification (LLOQ = 1.95 µg/l). Precision (CV %) and accuracy (% deviation from nominal concentration) were calculated for two replicates of three concentrations (7.8, 62.5 and 125 µg/l) on three different days. Precision was 10%, 2% and 2%, and accuracy 104%, 98%, and 99% for the three tested concentrations.

2.4. Permeation rate, lag time, and permeability coefficient

The cumulative amount of BPA in the receptor fluid per unit skin area was plotted over time for each skin sample (permeation curve). For each plot, the peak permeation rate (J_{peak} , µg/cm²/h) was calculated as the slope of the steepest linear portion of the permeation curve by fitting a piecewise linear model with an initial plateau and subsequent increase using a nonlinear regression model. The linear portion after the initial plateau was identified visually prior to the fitting. K_p was calculated using Fick's first law only for experiments where J reached a maximum constant value (steady state, J_{ss}). The lag time, or time needed to reach the steady state (t_{lag}), was calculated as the time (x-axis) intercept of the steady state portion of the permeation curve. When the steady state was not reached, the time to reach the peak permeation rate (apparent lag time) was calculated as the time (x-axis) intercept of the steepest linear portion of the permeation curve.

Table 2
Summary of BPA skin permeation experiments.

| Experiment | Concentration [mg BPA/l] | Vehicle volume [µl/cm ²] | Dose [µg/cm ²] | Skin donors [D] | Total skin samples [n] | Skin thickness [µm] | Skin state |
|-------------------|-----------------------------|---|-------------------------------|--------------------|---------------------------|------------------------|-----------------|
| EXP0 | 164 | 10 | 1.6 | 2 | 6 | 800 | Viable |
| EXP1 | 250 | 100 | 25 | 3 | 10 | 800 | Viable |
| EXP2 | 250 | 100 | 25 | 3 | 9 | 800 | Frozen (−80 °C) |
| EXP3 | 18 | 100 | 1.8 | 2 | 6 | 800 | Viable |
| EXP4 | 250 | 1000 | 250 | 3 | 10 | 800 | Viable |
| EXP5 ^a | 250 | 100 | 25 | 3 | 12 | 200 | Viable |
| EXP6 | 250 | 1000 | 250 | 1 | 3 | 200 | Viable |
| EXP7 | 250 | 1000 | 250 | 1 | 3 | 400 | Viable |

^a EXP5 data are reported here from Reale et al., (2020).

2.5. Statistical data analysis

The by-experiment estimates of J , K_p and t_{lag} were further analyzed as a function of several experimental parameters using a linear mixed-effect model. These parameters were skin state (viable vs. frozen), skin thickness, vehicle volume applied on skin, and BPA concentration applied on skin. Skin donor was used as a random effect. Restricted Maximum Likelihood was used to fit this mixed model. We report estimates and standard errors of J , K_p and t_{lag} obtained as predictions from this model. The difference in J , K_p and t_{lag} values due to the variation in one tested parameter was considered statistically significant when P value was <0.05 . Statistical data analysis was done using Stata/IC v. 14.0 (StataCorp LLC, TX, USA).

3. Results

Table 3 summarizes the results by paired comparisons between experiments differing by only one experimental parameter (Table 3, column "Experimental parameter for statistical analysis"): skin state (viable vs. frozen), vehicle concentration, vehicle volume, and skin thickness. The effects of vehicle concentration, vehicle volume and skin thickness were tested with viable skin. The reported results are the mean BPA amount in the receptor fluid (as % of the dose) after 24 h of exposure, as well as model-based estimates of J , t_{lag} , and K_p . These estimates take into account the within-donor correlation, which is highly influential given the uneven number of replicates for each donor. This is the reason why the results for the same experiments varied slightly across the

Table 3

Effect of different experimental parameters on BPA skin permeation kinetics. Model-based estimates (\pm se) are reported. Human skin was viable in all experiments except in EXP2.

| Experiment | Experimental parameter for statistical analysis | Vehicle volume [μ l] | Dose [μ g/ cm^2] | Skin thickness [μ m] | BPA in receptor fluid at 24 h [% of the dose] | J_{peak} [μ g/ cm^2/h] model-based estimate (\pm se) | P^a | $K_p \times 10^{-3}$ [cm/h] model-based estimate (\pm se) | P^a | t_{lag} [h] model-based estimate (\pm se) | P^a |
|--|---|---------------------------|---------------------------------|---------------------------|---|---|--------------------|--|--------------------|--|--------------------|
| EXP1 | Skin status Viable skin | 100 | 25 | 800 | 13 (\pm 8) | 0.14 (\pm 0.08) | <0.001 | NA | NA | 8.1 ^e (\pm 0.5) | 0.009 |
| EXP2 | Frozen skin | 100 | 25 | 800 | 24 (\pm 8) | 0.47 (\pm 0.08) | | NA | | 6.5 ^e (\pm 0.5) | |
| Vehicle concentration [mg/l] | | | | | | | | | | | |
| EXP1 | 250 | 100 | 25 | 800 | 13 (\pm 8) | 0.21 (\pm 0.06) | 0.041 | NA | NA | 8.0 ^e (\pm 2.2) | 0.947 |
| EXP3 | 18 | 100 | 1.8 | 800 | 16 (\pm 8) | 0.02 (\pm 0.07) | | NA | | 8.2 ^e (\pm 2.7) | |
| Vehicle volume [μl/cm^2] | | | | | | | | | | | |
| EXP1 | 100 | 100 | 25 | 800 | 13 (\pm 8) | 0.21 (\pm 0.08) | 0.078 ^g | NA | NA | 8.0 ^e (\pm 1.0) | 0.03 ^g |
| EXP4 | 1000 | 1000 | 250 | 800 | 2.0 (\pm 1.1) | 0.42 (\pm 0.08) ^f | | 1.66 (\pm 0.33) | | 11.1 (\pm 1.0) | |
| EXP5 ^b | 100 | 100 | 25 | 200 | 32 (\pm 12) | 0.72 (\pm 0.18) | 0.119 ^h | NA | NA | 3.9 ^e (\pm 0.4) | $<0.001^h$ |
| EXP6 | 1000 | 1000 | 250 | 200 | 8.4 (\pm 1.1) | 1.31 (\pm 0.31) ^f | | 5.25 (\pm 1.32) | | 8.3 (\pm 0.8) | |
| Skin thickness [μm] | | | | | | | | | | | |
| EXP1 | 800 | 100 | 25 | 800 | 13 (\pm 8) | 0.21 (\pm 0.15) | 0.013 ⁱ | NA | NA | 8.0 ^e (\pm 0.5) | $<0.001^i$ |
| EXP5 ^b | 200 | 100 | 25 | 200 | 32 (\pm 12) | 0.70 (\pm 0.14) | | NA | | 3.9 ^e (\pm 0.5) | |
| EXP4 | 800 | 1000 | 250 | 800 | 2.0 (\pm 1.1) | 0.41 (\pm 0.09) ^f | NA | 1.63 (\pm 0.36) | NA | 11.1 (\pm 1.2) | NA |
| EXP7 | 400 | 1000 | 250 | 400 | 3.1 (\pm 1.7) | 0.49 (\pm 0.15) ^f | 0.614 ^c | 1.94 (\pm 0.58) | 0.614 ^c | 7.5 (\pm 1.8) | 0.021 ^c |
| EXP6 | 200 | 1000 | 250 | 200 | 8.4 (\pm 1.1) | 1.31 (\pm 0.15) ^f | $<0.001^d$ | 5.23 (\pm 0.58) | $<0.001^d$ | 7.7 (\pm 1.8) | 0.032 ^d |

NA, not available.

^a P value calculated from Restricted Maximum Likelihood statistical analysis.

^b EXP5 data are reported here from Reale et al. (2020).

^c P values calculated comparing EXP7 with EXP4 (400 versus 800 μ m skin thickness).

^d P values calculated comparing EXP6 with EXP4 (200 versus 800 μ m skin thickness).

^e Apparent lag times.

^f J_{ss} .

^g P values calculated comparing EXP1 with EXP4 (100 versus 1000 μ l of vehicle volume for 800 μ m skin thickness).

^h P values calculated comparing EXP5 with EXP6 (100 versus 1000 μ l of vehicle volume for 200 μ m skin thickness).

ⁱ P values calculated comparing EXP5 with EXP1 (200 versus 800 μ m skin thickness for 100 μ l of vehicle volume).

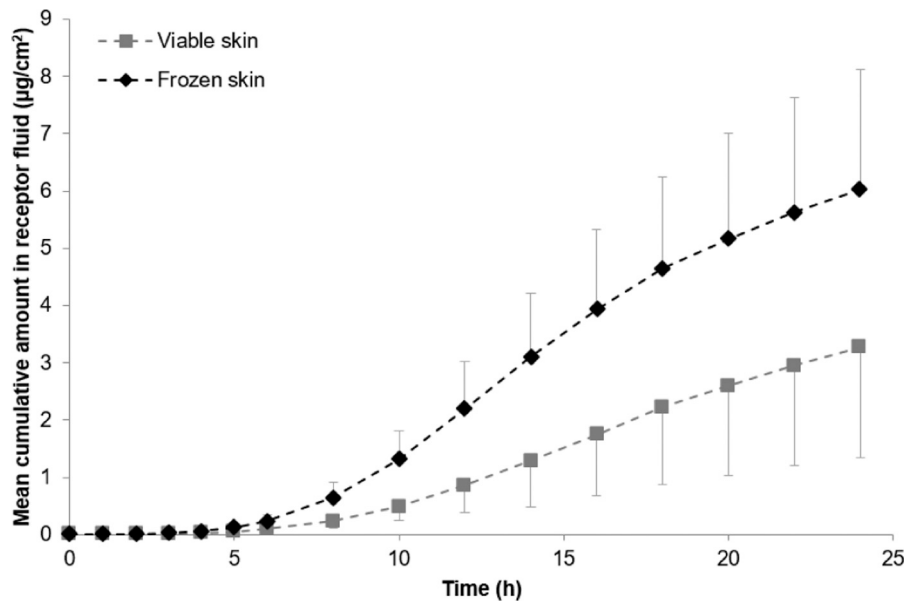


Fig. 1. Effect of freezing skin on BPA skin permeation: comparison of BPA mean skin permeation curves for 800 μm -thick viable (EXP1) and frozen (EXP2) skin during 24 h of exposure to 25 $\mu\text{g}/\text{cm}^2$ of BPA. One-sided error bars (SD) are shown in the figure for clarity purposes.

comparisons (e.g. J_{peak} for EXP1 was 0.14 and 0.21 for skin status and vehicle concentration, respectively).

The effects that the studied experimental parameters had on BPA mean skin permeation curves are shown in Figs. 1 to 4. Mean permeation curves were calculated over total skin samples used for experiments EXP1 to EXP7. EXP0 of Table 2 was not compared statistically because it differed by two or more parameters with any other experiment. The mean (\pm SD) J_{peak} value for EXP0 was 0.006 (\pm 0.003) ($n = 6$) (permeation curve not shown). It is worth noting that in the paired comparisons where vehicle volume changed, either the dose or the concentration also needed to change. We opted to keep concentration constant, as it is directly related to J , which is the parameter we compared across experiments.

Mean BPA permeation curves for viable and frozen skin are compared in Fig. 1. Human skin previously frozen at -80°C had 3.4-fold

higher J ($P < 0.001$) compared to viable skin. Mean BPA permeation curves for different BPA concentrations are shown in Fig. 2. A 14-fold increase in applied BPA concentration (18 vs. 250 mg/l) led to a 10.5-fold increase in J ($P < 0.05$), as expected since J is dependent on the permeant's concentration. Mean BPA permeation curves for different vehicle volumes are shown in Fig. 3. The curves show that J reached a maximum constant value, i.e. J_{ss} , only in the experiment where 1000 μl of vehicle were applied on the skin. A volume increase from 100 to 1000 μl led to a non-significant increase in J both with 800 and 200 μm -thick skin ($P = 0.078$ and 0.119, respectively). Fig. 4 shows the mean skin permeation curves of BPA through human skin dermatomed at 800 μm and at 200 μm , both for 100 and 1000 μl vehicle volume. With 100 μl vehicle volume, a decrease in skin thickness from 800 μm to 200 μm led to a 3.3-fold increase ($P = 0.013$) of BPA's J . With 1000 μl of vehicle volume, a decrease in skin thickness from 800 μm to 200 μm led to a 3.2-

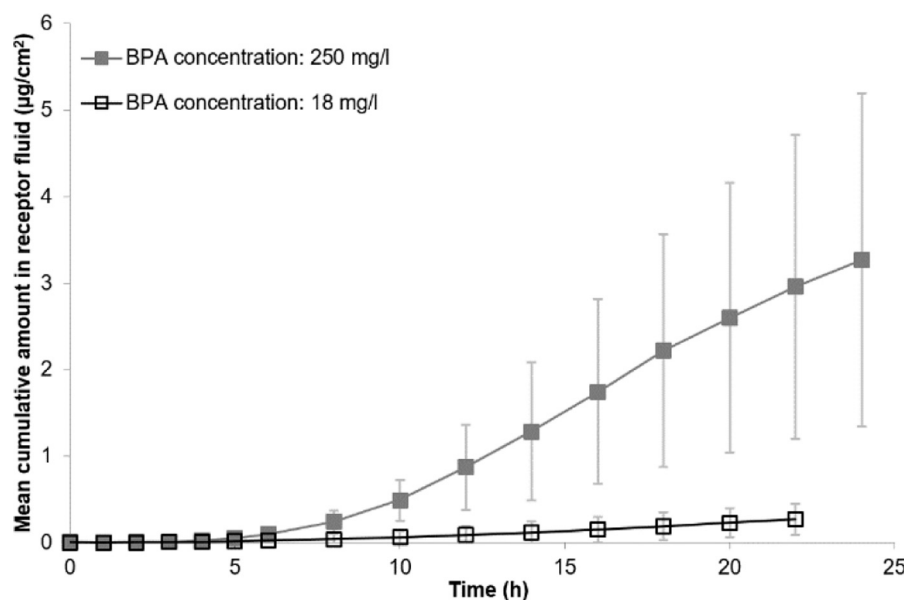


Fig. 2. Effect of BPA concentration in the vehicle applied on the skin on BPA skin permeation: comparison of BPA mean (\pm SD) skin permeation curves for 250 mg/l (EXP1) vs. 18 mg/l (EXP3) during 24 h of exposure. Vehicle volume added on the skin was 100 $\mu\text{l}/\text{cm}^2$.

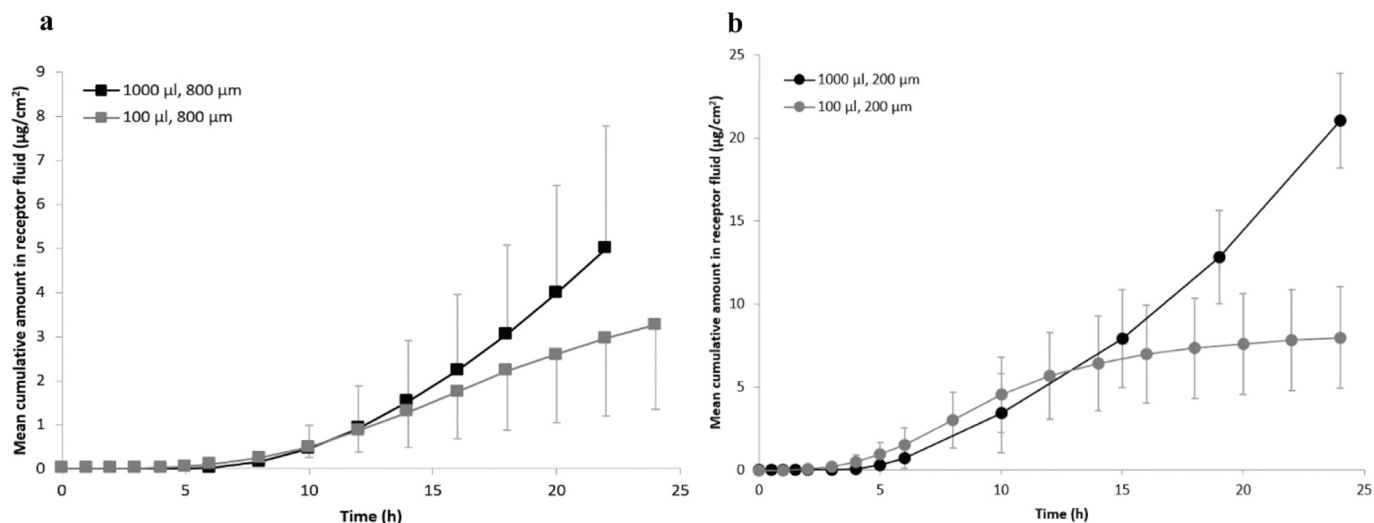


Fig. 3. Effect of vehicle volume applied on viable skin on mean BPA skin permeation curves of 800- μm (a) (EXP1, EXP4) and 200- μm -thick skin (b) (EXP5, EXP6) during 24 h of exposure. One-sided error bars (SD) are shown on fig. A for clarity purposes. EXP5 data were extracted from Reale et al. (2020). Note the different scale on the y-axes.

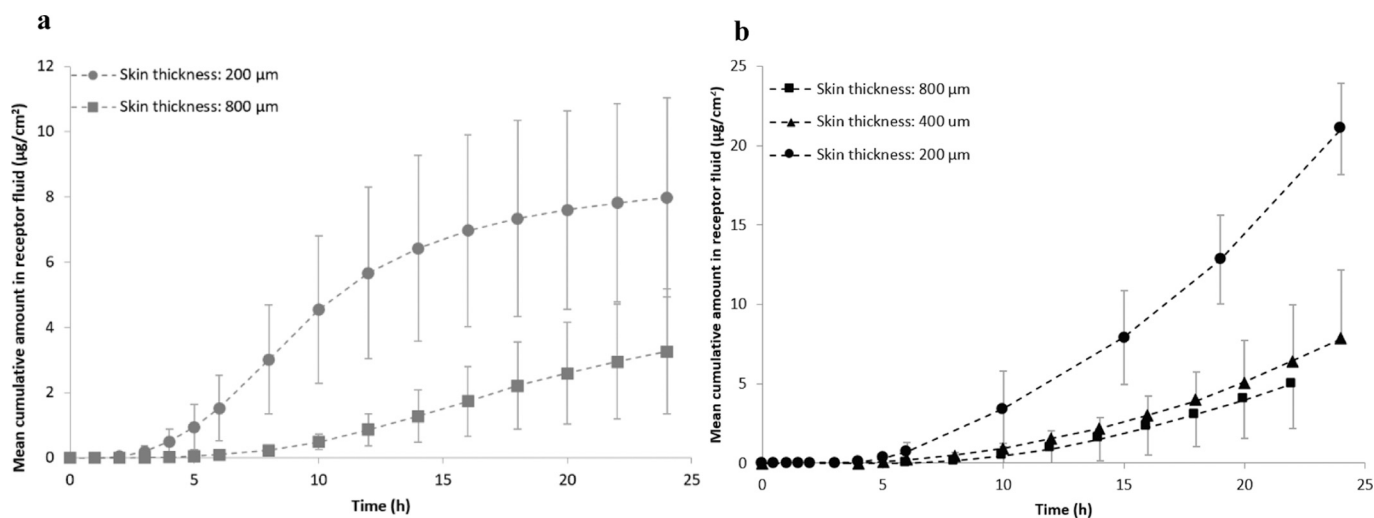


Fig. 4. Effect of skin thickness on BPA mean (\pm SD) permeation curves during 24 h of exposure to 100 μl (a) (EXP1, EXP5) and 1000 μl (b) (EXP 4, EXP6, EXP7) vehicle volume. EXP5 data were extracted from Reale et al. (2020).

fold increase ($P < 0.001$) of J , while a decrease in skin thickness from 800 to 400 μm led to a non-significant increase in J (0.614). The amount of BPA detected in the receptor fluid after 24 h of exposure was more than double for the 200 μm -thick skin, compared to the 400 and 800 μm -thick skin.

4. Discussion

We studied the effect that different experimental parameters have on BPA skin permeation kinetics. Our results show that a skin thickness increase from 200 to 400/800 μm and viable/frozen skin state had the greatest significant effect on J . Neither a volume increase from 100 to 1000 μl nor a skin thickness increase from 400 to 800 μm significantly affected J . Applying 1000 μl of BPA dosing solution on the skin resulted in an infinite dose that led to the steady state after 7–11 h (t_{lag}) depending on the skin thickness. As for J , K_p decreased significantly with a skin thickness increase from 200 to 400/800 μm .

As expected, significant differences in J were found between experiments with different concentrations (EXP1 and EXP3). This difference was also observed between viable and frozen skin (EXP1 and EXP2).

Numerous studies have addressed the effect of skin storage, showing that storing human skin at -20°C does not have any effects on its barrier function (Dennerlein et al., 2013; Harrison et al., 1984; Moody et al., 2009; Williams, 2003). In our study, the skin was stored at -80°C . The increased permeability of skin frozen at -80°C is in contrast with some literature data (Barbero and Frasch, 2016) and in line with other studies (Hawkins and Reifenrath, 1984; Nielsen et al., 2011). Therefore, it is likely that freezing at -80°C is harsher on barrier function compared to -20°C .

J and K_p decreased significantly (3.3-fold) when the skin thickness increased from 200 μm to 400 and 800 μm . Although, the number of replicates ($n = 3$) is below the recommended value ($n = 4$) by OECD (OECD, 2004a) for EXP6 and EXP7, which is a clear limitation of this study, the permeation curves of skin samples with different skin thicknesses (200, 400, and 800 μm) from the same skin donor were similar to Fig. 4B (data not shown). Several explanations for the observed decrease in J and K_p for thicker skin are possible. K_p is inversely proportional to the path length across the skin, thus the thicker the skin, the longer the path length and the smaller the K_p . In addition, the stratum corneum is a lipid-rich environment compared to the watery viable epidermis and

dermis. For lipophilic substances such as BPA ($\log K_{OW} = 3.4$ (EC IHCP, 2010)), the epidermis and dermis may act as rate-limiting layers in the diffusion through the skin (Moss et al., 2015; Wilkinson et al., 2006). The main clearance of substances absorbed in the skin occurs where the majority of the skin's vasculature resides, in the dermis at its junction with the epidermis (Moss et al., 2015). In human abdominal skin, this junction is at approximately 70 μm from the skin surface (Rees and Robertson, 2010). Therefore, the use of thicker skin samples (400–800 μm) may lead to an underestimation of BPA skin permeation kinetics, but it may also allow the quantification of the BPA stored in the skin. BPA skin storage has been reported by several authors (13–15% of applied dose (Kaddar et al., 2008; Liu and Martin, 2019; Reale et al., 2020; Toner et al., 2018); 25% by Mörck et al. (2010); 42% by Zalko et al. (2011)). This storage could potentially lead to BPA post-exposure release.

EXPO shared the experimental setup with Demierre et al. (2012) with the exception of skin thickness (800 μm in EXPO vs. 200 μm in Demierre et al. (2012)), skin state (viable vs. frozen at -20°C), and a slightly different BPA concentration in the dosing solution (164 mg/l vs. 184 mg/l). Calculating a J for 200 μm by taking into account our result of a 3.3-fold increase in J with a skin thickness reduction from 800 to 200 μm , resulted in a J of 0.020, which is very similar to Demierre et al. (2012)'s results. Applying the 3.4-fold difference for skin state yielded 0.067 $\mu\text{g}/\text{cm}^2/\text{h}$, which is 3-fold higher than in Demierre et al. (2012). This may suggest that this factor applies only for skin frozen at -80°C , which was our freezing condition, but not for skin frozen at -20°C as in Demierre et al. (2012)'s study.

Our results showed that J did not vary significantly between 400 and 800 μm skin thickness. J values obtained in the EXPO experiment (800 μm skin thickness) and the in vitro flow-through diffusion cell study of Toner et al. (2018) (350–400 μm skin thickness) were in the same order of magnitude (0.006 $\mu\text{g}/\text{cm}^2/\text{h}$ in EXPO, 0.0034 in Toner et al. (2018)), despite differences in vehicle and receptor fluid (Toner et al. used phosphate buffered saline solution as vehicle and receptor fluid).

A volume increase from 100 to 1000 μl did not significantly change J for the 200- nor the 800- μm thick skin, despite the 10-fold difference in applied dose (25 vs. 250 $\mu\text{g}/\text{cm}^2$). This suggests that once the skin is sufficiently hydrated, increasing the water volume on the skin does not further affect the skin permeation. However, the skin permeation curve for the 100 μl vehicle volume experiment (EXP1 in Fig. 3A, and EXP5 in Fig. 3B for 800 μm and 200 μm -thick skin, respectively) showed a decrease after 12 h of exposure. Before 12 h, the curves were similar irrespective of volume applied and skin thickness. The decrease observed in the 100 μl skin permeation curve's slope after 12 h of exposure could be due to effects arising from finite dosing and from total evaporation of the 100 μl vehicle from the skin (EFSA, 2015), which resulted in dryer, hence less permeable skin (Bunge et al., 2012; Frasch et al., 2014; Zhu et al., 2016).

A comparison of EXP5 and Demierre et al. (2012) suggests that the vehicle evaporation effect might be more important when comparing 100 μl with 10 μl of vehicle volume. EXP5 and Demierre et al. (2012)'s study shared the same experimental setup except for vehicle volume (100 μl vs. 10 μl), skin state (viable vs. frozen at -20°C), and BPA concentration in the dosing solution (250 mg/l vs. 184 mg/l). Despite the fact that Demierre et al. (2012)'s skin was frozen, their J value (0.022 $\mu\text{g}/\text{cm}^2/\text{h}$) was 30-fold smaller than that of EXP5 (0.72 $\mu\text{g}/\text{cm}^2/\text{h}$). This difference in J values was likely to be due to the difference in vehicle volume, rather than the slight difference in concentration. In experiments where 10 $\mu\text{l}/\text{cm}^2$ of water vehicle are used, the vehicle volume is so small that it is barely visible on the skin; when 100 $\mu\text{l}/\text{cm}^2$ of water vehicle are used, the skin is completely covered by the vehicle for several hours. Water increases skin hydration, which is known to increase skin permeability of other compounds. When comparing the application of 10 $\mu\text{l}/\text{cm}^2$ and 100 $\mu\text{l}/\text{cm}^2$, our J values for BPA were 30-fold greater for the larger vehicle volume.

The role of vehicle volume on BPA skin permeation kinetics is

probably more important for water than for other commonly used vehicles, as BPA permeates more readily through the skin when applied in aqueous vehicle, compared to acetone or sebum (Champmartin et al., 2020). Champmartin et al. (2020) studied the effects of vehicle type on BPA skin permeation, and observed that BPA permeated human viable skin faster when vehicle was water > acetone > sebum. Furthermore, the BPA dose (20 $\mu\text{g}/\text{cm}^2$ in 50 μl of 400 mg/l BPA solutions) through 476 μm -thick skin was infinite in acetone and sebum vehicles, and finite in water vehicle. As BPA readily permeates the skin when vehicle is water, dose conditions (100 $\mu\text{g}/\text{cm}^2$ of a saturated solution) ten-fold higher than the ones recommended by the (OECD, 2004a) were not enough to reach the steady-state in our study. This difficulty in maintaining infinite dose conditions has been observed also for other lipophilic substances (Selzer et al., 2013). In our study, steady state conditions were achieved and BPA's K_p could be calculated only for EXP 4, 6, and 7 where 1000 μl vehicle volume was applied. The higher J_{ss} and K_p values were observed for the thinner skin samples (200 μm , EXP6), which was expected as previously discussed.

No direct comparison of our J values with those of Marquet et al. (2011), Champmartin et al. (2020), and Liu and Martin (2019) was possible because too many parameters were different: vehicle volume and type, diffusion system, BPA concentration, skin thickness, and receptor fluid. Moreover, Liu and Martin (2019) used an in vitro 3D-skin model (120 μm thickness) with custom permeation devices and approximately 1500 $\mu\text{l}/\text{cm}^2$ of low concentration dosing solutions (1 and 5 mg/l). These particular conditions led to a plateau in BPA permeation curve indicating finite dose conditions.

In risk assessment and in toxicokinetic modelling, a substance's absorbed amount (expressed as percent of the applied dose) is often used to calculate the internal dose. However, the dependence of BPA's absorbed amount on the experimental set up is unclear. Here, we propose to use J values that correspond to different exposure scenarios. A cashier touching thermal paper receipts several times per day has a fairly constant amount of BPA on the skin all day long (Biedermann et al., 2010). BPA migrates onto the cashier's skin in solid phase, and, to be absorbed must be dissolved in sebum, sweat or other liquids. Average sweat output is approximately 2 $\mu\text{l}/\text{cm}^2$ (Misra et al., 2010), and average BPA migrated on the skin from thermal paper is 1.1 $\mu\text{g}/\text{cm}^2$ (Biedermann et al., 2010). BPA migration onto humid or greasy skin can be ten times higher than on dry/normal skin (Biedermann et al., 2010). Therefore, a J value for 10 μl vehicle volume, 200 μm -thick, viable skin (approximately 0.02 cm/h) could represent a scenario where the person touching the receipts has dry hands. K_p and J values for 1000 μl water vehicle volume, 200 μm -thick, viable skin (5.2×10^{-3} cm/h and 1.31 $\mu\text{g}/\text{cm}^2/\text{h}$, respectively), could represent the worst-case scenario of a person with wet hands.

5. Conclusions

Overall, comparison among a few studies shows that the different results of different experimental set ups agree with each other. The difference in the results depends on some experimental parameters, such as skin thickness and the vehicle volume. The use of thinner skin (200 μm) may be appropriate for in vitro skin permeation kinetic studies of BPA, and the use of thicker skin (400–800 μm) for in vitro mass balance studies to account for possible storage effect in the skin. Different vehicle volumes could represent different exposure scenarios with dry and wet hands' skin. For dry (normal) skin, Demierre et al. (2012)'s J value of 0.022 $\mu\text{g}/\text{cm}^2/\text{h}$ may be used. For exposure scenarios where hands are wet, the worst-case scenario is represented by the steady state J_{ss} and K_p values of 1.31 $\mu\text{g}/\text{cm}^2/\text{h}$ and 5.23×10^{-3} cm/h, respectively.

Declaration of Competing Interest

This study was funded by the Swiss Federal Office of Public Health (FOPH) and the Swiss Centre for Applied Human Toxicology (SCAHT).

The authors declare that they have no conflicts of interest. The research data of this study are available under request.

Acknowledgements

We acknowledge the Centre Hospitalier Universitaire Vaudois (CHUV, Lausanne, Switzerland) for providing the human skin samples. Finally, we acknowledge Nicole Charrière for her help in the skin permeation assays, and Simon Deslarzes, Ferdinando Storti and Grégory Plateel of the Center universitaire romand de médecine légale for their help in the chemical analyses.

References

- ANSES, 2013. *Anses 2013 - Evaluation des risques du bisphénol A pour la santé humaine*.
 Barbero, A.M., Frasch, H.F., 2016. Effect of frozen human epidermis storage duration and cryoprotectant on barrier function using two model compounds. *Skin Pharmacol. Physiol.* 29, 31–40. <https://doi.org/10.1159/000441038>.
 Biedermann, S., Tschudin, P., Grob, K., 2010. Transfer of bisphenol a from thermal printer paper to the skin. *Anal. Bioanal. Chem.* 398, 571–576. <https://doi.org/10.1007/s00216-010-3936-9>.
 Bronaugh, R., Maibach, H., 2005. Percutaneous Absorption: Drugs, Cosmetics, Mechanisms, Methodology. <https://doi.org/10.1201/9780849359033>.
 Bunge, A.L., Persichetti, J.M., Payan, J.P., 2012. Explaining skin permeation of 2-butoxyethanol from neat and aqueous solutions. *Int. J. Pharm.* 435, 50–62. <https://doi.org/10.1016/j.ijpharm.2012.01.058>.
 Champmartin, C., Marquet, F., Chedik, L., Décret, M.-J., Aubertin, M., Ferrari, E., Grandclaude, M.-C., Cosnier, F., 2020. Human in vitro percutaneous absorption of bisphenol S and bisphenol A: a comparative study. *Chemosphere* 252, 126525. <https://doi.org/10.1016/j.chemosphere.2020.126525>.
 Demierre, A.-L., Peter, R., Oberli, A., Bourqui-Pittet, M., 2012. Dermal penetration of bisphenol A in human skin contributes marginally to total exposure. *Toxicol. Lett.* 213, 305–308. <https://doi.org/10.1016/j.toxlet.2012.07.001>.
 Dennerlein, K., Schneider, D., Göen, T., Schaller, K.H., Drexler, H., Korinth, G., 2013. Studies on percutaneous penetration of chemicals - impact of storage conditions for excised human skin. *Toxicol. in Vitro* 27, 708–713. <https://doi.org/10.1016/j.tiv.2012.11.016>.
 EFSA, 2015. Scientific opinion on the risks to public health related to the presence of bisphenol A (BPA) in foodstuffs. *EFSA J.* 13, 3978. <https://doi.org/10.2903/j.efsa.2015.3978>.
 EFSA, 2018. Call for Data Relevant to the Hazard Assessment of Bisphenol A (BPA) [WWW Document]. URL: <https://www.efsa.europa.eu/sites/default/files/engage/180309.pdf>.
 European Commission, Joint Research Centre, Institute for Health and Consumer Protection, 2010. *European Union Risk Assessment Report - Environment Addendum of April 2008 - 4,4'-ISOPROPYLIDENEDIPHENOL (BISPHENOL-A) - Part 1 Environment*. EU RAR.
 Frasch, H.F., Barbero, A.M., Dotson, G.S., Bunge, A.L., 2014. Dermal permeation of 2-hydroxypropyl acrylate, a model water-miscible compound: effects of concentration, thermodynamic activity and skin hydration. *Int. J. Pharm.* 460, 240–247. <https://doi.org/10.1016/j.ijpharm.2013.11.007>.
 Gundert-Remy, U., Mielke, H., Bernauer, U., 2013. Commentary: dermal penetration of bisphenol A—consequences for risk assessment. *Toxicol. Lett.* 217, 159–161. <https://doi.org/10.1016/j.toxlet.2012.12.009>.
 Harrison, S.M., Barry, B.W., Dugard, P.H., 1984. Effects of freezing on human skin permeability. *J. Pharm. Pharmacol.* 36, 261–262. <https://doi.org/10.1111/j.2042-7158.1984.tb04363.x>.
 Hawkins, G.S., Reifenrath, W.G., 1984. Development of an in vitro model for determining the fate of chemicals applied to skin. *Fundam. Appl. Toxicol.* 4, S133–S144. [https://doi.org/10.1016/0272-0590\(84\)90145-3](https://doi.org/10.1016/0272-0590(84)90145-3).
 Hormann, A.M., vom Saal, F.S., Nagel, S.C., Stahlhut, R.W., Moyer, C.L., Ellersieck, M.R., Welshons, W.V., Toutain, P.-L., Taylor, J.A., 2014. Holding thermal receipt paper and eating food after using hand sanitizer results in high serum bioactive and urine total levels of Bisphenol A (BPA). *PLoS One* 9. <https://doi.org/10.1371/journal.pone.0110509>.
 Kaddar, N., Harthé, C., Déchaud, H., Mappus, E., Pugeat, M., 2008. Cutaneous penetration of Bisphenol A in pig skin. *J. Toxicol. Environ. Health A* 71, 471–473. <https://doi.org/10.1080/15287390801906824>.
 Karrer, C., Roiss, T., von Goetz, N., Gramac Skledar, D., Peterlin Mašič, L., Hungerbühler, K., 2018. Physiologically based pharmacokinetic (PBPK) Modeling of the Bisphenols BPA, BPS, BPF, and BPAF with new experimental metabolic parameters: comparing the pharmacokinetic behavior of BPA with its substitutes. *Environ. Health Perspect.* 126, 077002 <https://doi.org/10.1289/EHP2739>.
 Kasting, G.B., 2001. Kinetics of finite dose absorption through skin 1. Vanillynonamide. *J. Pharm. Sci.* 90, 202–212. [https://doi.org/10.1002/1520-6017\(200102\)90:2<202::aid-jps11>3.0.co;2-e](https://doi.org/10.1002/1520-6017(200102)90:2<202::aid-jps11>3.0.co;2-e).
 Liu, J., Martin, J.W., 2019. Comparison of Bisphenol A and Bisphenol S percutaneous absorption and biotransformation. *Environ. Health Perspect.* 127, 67008 <https://doi.org/10.1289/EHP5044>.
 Marquet, F., Payan, J.-P., Beydon, D., Wathier, L., Grandclaude, M.-C., Ferrari, E., 2011. In vivo and ex vivo percutaneous absorption of [14C]-bisphenol A in rats: a possible extrapolation to human absorption? *Arch. Toxicol.* 85, 1035–1043. <https://doi.org/10.1007/s00204-011-0651-z>.
 Mielke, H., Gundert-Remy, U., 2009. Bisphenol A levels in blood depend on age and exposure. *Toxicol. Lett.* 190, 32–40. <https://doi.org/10.1016/j.toxlet.2009.06.861>.
 Mielke, H., Gundert-Remy, U., 2012. Physiologically based toxicokinetic modelling as a tool to support risk assessment: three case studies. *J. Toxicol.* 2012, 1–11. <https://doi.org/10.1155/2012/359471>.
 Misra, U.K., M., Al, E., 2010. *Clinical Neurophysiology*, 2Nd edition. Elsevier India.
 Moody, R.P., Yip, A., Chu, L., 2009. Effect of cold storage on in vitro human skin absorption of six 14C-radiolabeled environmental contaminants: Benzo[a]Pyrene, ethylene glycol, methyl parathion, naphthalene, nonyl phenol, and toluene. *J. Toxicol. Environ. Health A* 72, 505–517. <https://doi.org/10.1080/15287390802328713>.
 Mørck, T.J., Sorda, G., Bechi, N., Rasmussen, B.S., Nielsen, J.B., Ietta, F., Rytting, E., Mathiesen, L., Paulesu, L., Knudsen, L.E., 2010. Placental transport and in vitro effects of Bisphenol A. *Reprod. Toxicol.* 30, 131–137. <https://doi.org/10.1016/j.reprotox.2010.02.007>.
 Moss, G., Gullick, D., Wilkinson, S., 2015. *Predictive Methods in Percutaneous Absorption*. Springer-Verlag, Berlin Heidelberg. <https://doi.org/10.1007/978-3-662-47371-9>.
 Ndaw, S., Remy, A., Jargot, D., Robert, A., 2016. Occupational exposure of cashiers to Bisphenol A via thermal paper: urinary biomonitoring study. *Int. Arch. Occup. Environ. Health* 89, 935–946. <https://doi.org/10.1007/s00420-016-1132-8>.
 Nielsen, J.B., Plasencia, I., Sørensen, J.A., Bagatolli, L.A., 2011. Storage conditions of skin affect tissue structure and subsequent in vitro percutaneous penetration. *Skin Pharmacol. Physiol.* 24, 93–102. <https://doi.org/10.1159/000322304>.
 OECD, 2003. *OECD Existing Chemicals Database - Bisphenol A* [WWW Document]. URL: https://hpvchemicals.oecd.org/UI/SIDS_Details.aspx?key=6d209d66-9690-4739-8745-ac4732d5f53d&idx=0 (accessed 11.20.19).
 OECD, 2004a. *Organisation for Economic Co-operation and Development, Guidelines for the testing of chemicals, Section 4, Test N° 428: Skin absorption: In Vitro Method*.
 OECD, 2004b. *Organisation for Economic Co-operation and Development, Series on Testing and Assessment N° 28, Guidance Document for the Conduct of Skin Absorption Studies*. OECD. <https://doi.org/10.1787/9789264078796-en>.
 OECD, 2011. *Organisation for Economic Co-operation and Development, Series on Testing and Assessment N° 156, Guidance Notes on Dermal Absorption*.
 Peretz, J., Vrooman, L., Ricke, W.A., Hunt, P.A., Ehrlich, S., Hauser, R., Padmanabhan, V., Taylor, H.S., Swan, S.H., VandeVoort, C.A., Flaws, J.A., 2014. Bisphenol A and reproductive health: update of experimental and human evidence, 2007–2013. *Environ. Health Perspect.* 122, 775–786. <https://doi.org/10.1289/ehp.1307728>.
 Pinnagoda, J., Tupker, R.A., Agner, T., Serup, J., 1990. Guidelines for transepidermal water loss (TEWL) measurement. A report from the standardization Group of the European Society of contact dermatitis. *Contact Derm.* 22, 164–178. <https://doi.org/10.1111/j.1600-0536.1990.tb01553.x>.
 Reale, E., Vernez, D., Hopf, N.B., 2020. Skin absorption of Bisphenol A and its alternatives in thermal paper. *Ann. Work Expo. Health.* <https://doi.org/10.1093/annweh/wxaa095>.
 Rees, J., Robertson, K., 2010. Variation in epidermal morphology in human skin at different body sites as measured by reflectance confocal microscopy. *Acta Derm. Venerol.* 90, 368–373. <https://doi.org/10.2340/00015555-0875>.
 Selzer, D., Abdel-Mottaleb, M.M.A., Hahn, T., Schaefer, U.F., Neumann, D., 2013. Finite and infinite dosing: difficulties in measurements, evaluations and predictions. In: *Advanced Drug Delivery Reviews, Modeling the human skin barrier - Towards a Better Understanding of Dermal Absorption*, 65, pp. 278–294. <https://doi.org/10.1016/j.addr.2012.06.010>.
 Toner, F., Allan, G., Dimond, S.S., Waechter, J.M., Beyer, D., 2018. In vitro percutaneous absorption and metabolism of Bisphenol A (BPA) through fresh human skin. *Toxicol. in Vitro* 47, 147–155. <https://doi.org/10.1016/j.tiv.2017.11.002>.
 US EPA, 2014. *Bisphenol A Alternatives in Thermal Paper, Final Report*. Environmental Protection Agency, United States.
 Völkel, W., Colnot, T., Csanády, G.A., Filsler, J.G., Dekant, W., 2002. Metabolism and kinetics of bisphenol a in humans at low doses following oral administration. *Chem. Res. Toxicol.* 15, 1281–1287.
 Wilkinson, S.C., Maas, W.J.M., Nielsen, J.B., Greaves, L.C., van de Sandt, J.J.M., Williams, F.M., 2006. Interactions of skin thickness and physicochemical properties of test compounds in percutaneous penetration studies. *Int. Arch. Occup. Environ. Health* 79, 405–413. <https://doi.org/10.1007/s00420-005-0056-5>.
 Williams, A., 2003. *Transdermal and Topical Drug Delivery from Theory to Clinical Practice*. Pharmaceutical Press.
 Zalko, D., Jacques, C., Duplan, H., Bruel, S., Perdu, E., 2011. Viable skin efficiently absorbs and metabolizes bisphenol a. *Chemosphere* 82, 424–430. <https://doi.org/10.1016/j.chemosphere.2010.09.058>.
 Zhu, H., Jung, E.-C., Hui, X., Maibach, H., 2016. Proposed human stratum corneum water domain in chemical absorption. *J. Appl. Toxicol.* 36, 991–996. <https://doi.org/10.1002/jat.3208>.